Some exploratory experiments with a new type of rotating, differentially-heated fluid annulus

By PETER A. DAVIES[1] and GÖSTA WALIN,[2] *International Meteorological Institute, University of Stockholm*[3]

(Manuscript received August 26, 1974; in final form April 2, 1975)

ABSTRACT

Some experiments with a rotating differentially heated annulus are presented. It is demonstrated that with suitable construction of the annulus the strength of the zonal baroclinic motion may be chosen independently of the basic density stratification. In the experiment reported it was found that baroclinic instability occurred in a state characterized by small isotherm slopes. Certain aspects of the observed flow and temperature fields—in particular the basic stratification and the slope of the isotherms—are compared with approximate theoretical predictions. Certain basic difficulties associated with the sensitivity of the baroclinic flow to small changes in the boundary conditions are discussed.

1. Introduction

Since the late 1950's when Hide (1958) and Fultz (1959) performed experiments with a rotating, differentially-heated fluid annulus, great efforts, both experimental and theoretical, have been made to understand the observed fluid behaviour. In this connection, the 'classical' experimental annulus, which rotates about a vertical axis with angular velocity, Ω, is formed between two concentric cylinders made of perfectly heat conducting material, across which a horizontal temperature difference ΔT is impressed. (There is no differential rotation of one cylinder with respect to the other.) With this arrangement, it is observed that several distinct flow regimes can occur, the boundaries between each regime being mainly determined by the values of Ω and ΔT. The particular transition between the stable axisymmetric regime and the regular baroclinic wave regime has stimulated keen theoretical interest in the problem in view of the important role played by the baroclinic instability mechanism in much of the dynamics and energetics of the earth's atmosphere. A rather well-defined stability boundary between the various flow regimes has now been established as a result of a series of very careful experimental investigations (Fowlis & Hide, 1965; Fultz et al., 1959; Kaiser, 1969, 1970) and much additional knowledge of the detailed structure of the flows has been obtained (Hide & Mason, 1970; Douglas et al., 1972; Fultz & Kaiser, 1971; Pfeffer et al., 1970; Ketchum, 1972; Koschmeider, 1972).

The experiments to be described are related to the above studies and can be regarded as extensions of them. Their prime purpose has been to try and determine how the various characteristics (e.g. temperature and velocity fields, stability) of the fluid behaviour are affected by changes in the boundary conditions of the system, and how some of these changes compare with theoretical prediction. Specifically, the annulus walls are chosen to have a particular form and thickness and to be constructed of a material having a thermal conductivity intermediate between that of a typical metal and a typical thermal insulator. The reasons for choosing such boundaries arise from a theoretical study of a closely-related non-rotating problem (Walin, 1971, hereafter called I).

[1] Present address: Department of Geophysics and Planetary Physics, School of Physics, University of Newcastle upon Tyne, U.K.

[2] Present address: University of Gothenburg, Department of Oceanography, Box 4038, 400 40 Gothenburg, Sweden.

[3] Contribution no. 303.

In the non-rotating case Walin considered the problem of determining the density field in a fluid region enclosed by a container of arbitrary shape and thermal properties, from the prescribed boundary conditions applied at the wall of this container. Using a boundary-layer approach it was shown that the interior density field $\varrho^I(z, t)$ could be predicted within a certain (physically realistic) range of validity. Although Walin considered only non-rotating systems his analysis may be directly used to predict the basic stratification $\varrho^I(z, t)$ in rotating cases also, so long as the slopes of the isotherms are small. In particular it was shown that, under certain conditions, a given stratification could be obtained in the fluid interior merely by allowing the thickness of the boundary material to vary with height. In the present experiments the intention has been to use this result to set up a given stratification in an annulus having specially-constructed boundaries and then to investigate the fluid behaviour as this annulus is rotated.

With the arrangement chosen we obtain a system which without rotation has essentially a stagnant stratified core. When this system is rotated it becomes unstable, while the stratification is still undestroyed, i.e. when $\partial\varrho^I/\partial r \ll \partial\varrho^I/\partial z$. In this respect the system is essentially different from the classical arrangement in which the isotherm slope is always of order unity. It is hoped that these new features of the experiment will open new possibilities for relevant comparison with theoretical descriptions of the axisymmetric flow and its stability. It also seems that the case when the system is strongly stratified, i.e. when $\partial\varrho^I/\partial r \ll \partial\varrho^I/\partial z$, is of somewhat greater geophysical interest.

In section 2 the theoretical background to the problem is described. The essential features of the results in I are stated and the application of these results to the annulus configuration of the present experiments is developed. Following over to the case where the annulus is rotating, expressions for the basic stratification and the buoyancy layer flux are explicitly derived in terms of the physical properties of wall material and fluid and the thermal boundary conditions. The interesting result that the basic stratification can be fixed and the boundary layer flux (and hence the forcing of the system as shown, for example, by the tilt of the isotherms) varied independently of this stratification is revealed as a consequence of this derivation.

After a description of the experimental apparatus in section 3 the main results of the work are described. As shown, the intention in these experiments has not been simply to repeat the already-extensive classical annulus investigations of other workers but to follow a different approach based on certain specific theoretical predictions. However, the relevance of this previous work has naturally been borne in mind when studying, particularly, the stability of the symmetric flow in section 4.3. In this section the basic question of whether regular baroclinic wave motions develop in the annulus, under the special boundary conditions of the experiment, is investigated and the connection with the above-mentioned work is briefly discussed. In section 4.4 the bulk of the investigation—the temperature measurements—is fully described and the results are compared with theoretical predictions. In the process of making this comparison a theoretical check is made on some earlier measurements (section 4.2) on the horizontal velocities in the fluid interior.

2. Theoretical background

The experiments described in this paper mainly represent an effort to obtain a completely controlled and predictable thermally forced baroclinic flow. Some rather modest success in this effort has been achieved: the observations made on the flow obtained experimentally are not in conflict with theoretical expectations as will be described in later sections. It has not however been possible to create a flow situation which may be quantitatively related to a theoretical description in an unambiguous way. The difficulties encountered are of course partly associated with analytical problems. It appears however that the more serious obstacle on the road towards a quantitative comparison with experiment is related to the extreme sensitivity of the baroclinic zonal flow to small changes in the boundary conditions. The theoretical background to this disturbing fact will be outlined in the following two sub-sections. In order to limit the length of this discussion (and hopefully to make it readable) the treatment will rely to some extent on the reader's and our own physical intuition rather than on a formal analysis, leaving a more rigorous development to be presented separately, at a later date.

Non-rotating

Let us start with a description of the mechanics of our system when it is not rotating. The formal background to the present discussion may be found in I.

Our task in the non-rotating case is to describe the basic density (i.e. temperature) field and the associated meridional circulation.

Essentially the whole system may be described as an almost stagnant, stratified core surrounded by boundary layers on all sides, in which a certain transport, m^B, is carried around the core region.

Comparing with a similar system in which the fluid is enclosed by strongly conducting walls of constant thickness we note, in particular, the following characteristics of the system under consideration here.

(i) The meridional circulation is much weaker.

(ii) The boundary layers are laminar and governed by linear mechanics.

(iii) The motions in the core are far too weak to produce any appreciable horizontal temperature gradients; i.e. we are dealing with a truly stratified system.

As described in I these features are associated with the choice of boundary conditions; i.e. the semi-conducting walls with height-dependent thickness.

The two most important observables of our system are:

(i) The strength of the stratification, $\varrho^I(z)$, in the core region (R^I in Fig. 1).

(ii) The magnitude of the transport, m^B, carried by the boundary layer (see Fig. 1).

An important consequence of the analysis in I is that $\varrho^I(z)$ and m^B are determined independently. If, for example, the shape of the side walls is fixed, the stratification is essentially determined by the external temperature difference $(T_1 - T_2)$, while the transport m^B is determined by the conductivity of the walls facing the hot and cold baths.

Let us now discuss the characteristics of the various regions indicated in Fig. 1, limiting ourselves to the case

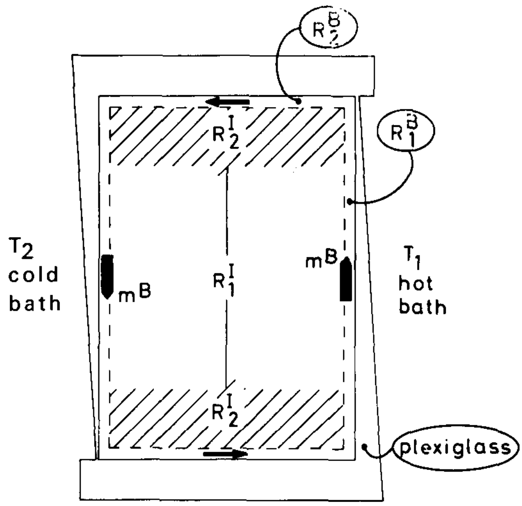

Fig. 1. Cross section of the annulus showing the major regions to be expected in the fluid.

$$1 \ll sH \ll \varepsilon^{-1} \tag{2.1}$$

Here, s is defined by the side wall boundary condition $\mathbf{n}\cdot\nabla\varrho = s(\varrho - \hat{\varrho})$ where $\mathbf{n}$ is the inward normal to the boundary, H is a typical length scale of the annulus. εH is a typical thickness of the side wall boundary layer, the so-called buoyancy layer (see I).

As discussed in I this is the regime most easily obtained experimentally; (2.1) being also reasonably well satisfied in our experiment.

In the main part R_1^I, of the core region R^I the density field $\varrho^I(z)$ (i.e. the temperature field) is determined by the condition that the total transport carried by the boundary layers through a level surface at height, z, should vanish. Since this transport depends on $\varrho^I(z)$ this means that the interior density field has to adjust to a state such that the net boundary layer transport vanishes at each level. If, for example, the core temperature for some reason were lower than in steady state, the transport upwards on the warm side would exceed the downward transport on the cold side. As a consequence a downward flow would appear in the interior which, by lowering the isotherms advectively, would adjust the interior temperature distribution to its equilibrium state.

It should be emphasised that all the properties of region R_1^I *and* the boundary layers between R_1^I and the vertical walls are independent of the regions above and below (e.g. of the boundary conditions on the horizontal boundaries).

Meridional motions in the main core region, R_1^I, arise from two causes

(i) *Divergence of the boundary layer transport.* If the transport m^B varies vertically we expect an interior meridional transport of order m^B. Since m^B is constrained to vary in a similar way on the two sides of the region the resulting flow is strictly horizontal (to lowest order at least); i.e.

$$u^I \sim m^B/H \tag{2.2a}$$

$$w^I \ll m^B/H \tag{2.2b}$$

where u^I is the radial and w^I the vertical velocity component in R^I. The transport m^B is given by (see I)

$$m^B = s\varkappa(\varrho^I - \hat{\varrho})\left(\frac{\partial \varrho^I}{\partial z}\right)^{-1} \tag{2.3}$$

where $\varkappa$ is the heat diffusivity.

(ii) *Interior diffusion.* Although the interior heat balance in R_1^I, has no zero order influence on the distribution $\varrho^I(z)$, it still has to be satisfied. This balance will then serve to determine the vertical velocity in R_1^I as a function of z. From elementary scaling considerations we obtain

$$w^I \sim \varkappa/H \tag{2.4a}$$

From continuity we find, in general, a corresponding contribution to the horizontal velocity in R_1^I

$$u^I \sim \varkappa/H \tag{2.4b}$$

In the regime defined by (2.1) the velocity scale given by (2.2) is always much larger than the scale given by (2.4). The contribution from diffusion may however still be of importance in cases when the geometry is chosen such that m^B does not vary vertically (to lowest order).

In regions R_2^I (shaded in Fig. 1) the interior density field is not independent of internal diffusion. The thickness of these regions, s^{-1}, is precisely small enough for diffusion to be able to balance the advective effect of a vertical transport of order m^B. From continuity we obtain in general

$$u^I \sim m^B s \tag{2.5a}$$

$$w^I \sim m^B/H \tag{2.5b}$$

(recalling that the width and height of the annulus $\sim H$).

The boundary layer regions R_2^B facing the horizontal boundaries are quite complicated. However, the only information we need about them is the transport m^E carried over from one corner to the other. In steady state the boundary layer transport must be continuous at the corner. Thus we have:

$$m^E \sim m^B \tag{2.6}$$

If R^I is stratified throughout, i.e. if our linear description of the side wall boundary layer (as given in I) holds everywhere, the estimates given in (2.2)–(2.6) may be replaced by quantitative expressions for the meridional flow. This of course requires that the boundary conditions are known with sufficient accuracy. For our experiment the last condition was probably not well enough fulfilled.

Furthermore, in our experiment the horizontal boundaries were approximately insulated in which case the boundary layer theory breaks down at the top and bottom of the region. This means that even the estimates as given by (2.5) and (2.6) might be questionable. For the present qualitative discussion a detailed investigation of these complications does not seem justified. It should be kept in mind, however, for future experiments that the upper and lower boundary condition, though relatively unimportant for the control of $\varrho^I(z)$ has important local effects on the meridional circulation and thereby on the zonal motion throughout the annulus.

With rotation

If we allow the system to rotate it is obvious that the meridional circulation will force a zonal motion in the core region. The situation may be described intuitively as follows.

The buoyancy layers (essentially unaffected by rotation) force fluid up and down the warm and cold boundaries respectively. Thus, fluid has to cross over the annulus somehow to close the circulation. This may occur in the core region in which case a tangential Coriolis force appears. Or it may occur in the form of an Ekman layer transport which for its existence requires a zonal motion in the core region at least close to the upper and lower boundaries. The former type of forcing corresponds to an inhomogeneity in the zonal momentum equation, the latter type to an inhomogeneous boundary condition to the same equation.

The zonal velocity field thus forced will be associated with some slope of the isotherms; i.e. a modification of the density field $\varrho^I(z)$. This, in turn, changes the core density at the side walls which affects the buoyancy layer flux and thereby the whole meridional circulation. If this modification is small it may either be neglected or an iterative procedure may be adopted.

The important fact to notice, making such an approach possible, is that the strength of the meridional circulation is basically independent of the strength of the stratification for the type of system under consideration. The stratification is determined by the shape of the walls and by the difference in temperature between hot and cold baths. The strength of the meridional circulation depends essentially on s (i.e. the conductivity and thickness of the walls) as outlined in the previous sub-section. It is then conceptually possible to think of a procedure in which we start with a rotating and stratified system with very weak forcing (i.e. small s) and successively increase the forcing.

In this respect our experimental set up differs from the classical one. In the classical approach, with strongly conducting boundaries, the forcing and the stratification of the system are not independent: it is impossible to decrease the forcing without simultaneously decreasing the stratification.

In principle we are thus in a position where we could predict the baroclinic motion in the annulus with a linear theory, and in what follows we will discuss some properties of this prediction problem. We will find that in practice the experimental realization of a completely controlled system is associated with certain basic difficulties which might call for some further basic modifications of the approach.

Finally, it should be noticed that the limitation to small isotherm slopes does not rule out the interesting flow situations. Baroclinic instability is, for example, a phenomenon which occurs within this framework as demonstrated by our experiment.

The zonal momentum balance

We will now discuss the forcing of the zonal motion under the assumption that the basic density field and thus the meridional circulation is only slightly modified by rotation. The purpose of this discussion is firstly to check if, or under what conditions, such an approach is valid and secondly to derive some preliminary results regarding the character of the zonal motion resulting from various types of forcing.

Assuming steady state and cylindrical symmetry the zonal momentum balance becomes

$$\left(u^I \frac{\partial}{\partial r} + \frac{w^I \partial}{\partial z} + \frac{u^I}{r}\right) v^I + 2\Omega u^I = \nu \left(\nabla^2 - \frac{1}{r^2}\right) v^I \quad (2.7)$$

where v^I is the zonal velocity component, Ω the rate of rotation and ν the kinematic viscosity.

Assuming now that (u^I, w^I) are known from the analysis of the non-rotating system we find that equation (2.7) is a *linear* equation for the zonal motion v^I.

To determine the zonal velocity v^I we should proceed in principle as follows:

(i) Determine (u^I, w^I, ϱ^I) as in I, i.e. assuming $\partial\varrho^I/\partial r \ll \partial\varrho^I/\partial z$

(ii) Insert the fields (u^I, w^I) thus obtained into equation (2.7) and solve the resulting linear equation for v^I making use of appropriate boundary conditions (see below)

(iii) Insert the zonal velocity field thus obtained into the thermal wind equation (or whatever form of the horizontal vorticity balance is relevant) and determine a correction ϱ_1^I to the density field found under (i)

(iv) Check that $\varrho_1^I \ll \varrho^I$

(v) If better accuracy is required we may determine a correction to (u^I, w^I) and continue with an iterative procedure.

To find correct boundary conditions to (2.7) we note that the buoyancy layers on the vertical walls do not involve the zonal velocity, implying

$$v^I = 0 \text{ on the vertical boundaries} \quad (2.8\text{a})$$

The horizontal boundary layers, on the other hand, are "converted" to Ekman layers in the rotating case. The transport m^E of these layers is determined by the thermal properties of the system. The relation

$$m^E = -\frac{1}{2}\left(\frac{\nu}{\Omega}\right)^{1/2} v^I \qquad (2.8\,\text{b})$$

for the Ekman transport (Ekman 1905) thus provides an inhomogeneous boundary condition on v^I.

We will now use equations (2.7), (2.8) and the estimates given by (2.2)–(2.6) to derive some qualitative properties of the zonal flow.

Let us first ignore the inhomogeneous terms in (2.7). This means that we assume the boundary layer flux to be non-divergent and the interior density field to be linear throughout R^I. In principle such a situation may be achieved by appropriate choice of the thermal boundary conditions.

The amplitude of v^I is then determined by the boundary condition (2.8b). Making use also of (2.6) and (2.3) we find

$$v^I \sim s\varkappa E^{-1/2} \qquad (2.9)$$

where

$$E = \nu/2\Omega H^2$$

The shape of the distribution v^I in this case will be smooth except close to the corners where the boundary condition is discontinuous, as follows from the properties of the elliptic operator in (2.7).

Consider next the response to an interior forcing as given by (2.2). We first note that the only real forcing in (2.7) is given by the Coriolis term $2\Omega u^I$, while the dissipation—i.e. the adjustment to the boundary conditions—is provided by the friction term on the right-hand side of (2.7). Each of these two terms thus have to be of primary importance at least somewhere in the region. The "inertial" term, on the other hand, essentially produces a more or less pronounced distortion of the velocity distribution.

Assuming first that the Coriolis force and friction term are both of lowest order importance in (2.7) we obtain

$$2\Omega u^I \sim \nu v^I/H^2 \qquad (2.10)$$

The amplitude of v^I now depends on what estimate for u^I we adopt and which part of R^I we consider. The circumstances we want to elucidate are however demonstrated well enough by the case with a divergent buoyancy layer as given by (2.2), which we chose as being most representative. We thus obtain from (2.2), (2.3) and (2.10)

$$v^I \sim s\varkappa E^{-1} \qquad (2.11)$$

Let us now estimate the ratio R_0 of the first term in (2.7) and the Coriolis force assuming (2.11) to hold. We obtain

$$R_0 \sim \frac{v^I}{2\Omega H} \sim sH\frac{\varkappa}{\nu} \qquad (2.12)$$

Recalling that we have assumed $sH \gg 1$ we find that we are not in general allowed to assume $R_0 \ll 1$ which was tacitly assumed when deriving (2.11). In particular, if we find $R_0 \gg 1$ (as given by (2.12)) we must reject (2.11) (and the accompanying assumption).

The only alternative is that the Coriolis force is primarily balanced by the inertial term, i.e. that

$$v^I \sim 2\Omega H \qquad (2.13)$$

The estimate given by (2.13) is independent of the forcing. It represents an upper bound on the zonal velocity corresponding to conservation of angular momentum in the core. The correct estimate is thus given by the smaller of (2.11) and (2.13).

Obviously (2.7) cannot satisfy the side wall boundary conditions if we ignore the friction term. We thus expect some kind of interior boundary layer to appear. Intuitively we may describe the situation by following a fluid particle on its way from one side-wall to the other. On leaving the boundary layer the particle has essentially no zonal velocity. As the particle moves radially it is successively accelerated in accordance with the inviscid form of (2.7). The zonal velocity relative to the annulus will thus increase approximately linearly with radial distance from the wall. This continues until the particle is close enough to the opposite boundary for friction to be of importance. On the "downstream" side we thus obtain a "boundary layer" precisely thin enough for the friction term in (2.7) to be locally important. In this layer v^I will drop to zero as imposed by the boundary condition.

Let us now compare the strength of the zonal motion forced by the Ekman layer (2.9) and by the interior meridional circulation as given by (2.11) or (2.13). We then find that the zonal motion forced by the Ekman layer is considerably weaker, in fact by as much as a factor $E^{1/2}$ when (2.11) is valid. This result has some disturbing consequences for the performance and control of an experiment.

Knowing all the complications with inhomogeneous rotating flow experiments it is most natural to try to create the simplest possible system to exhibit certain desired features (in this case a baroclinic zonal motion). It appeared to the authors that this goal would be best achieved with a system as close as possible to the case in which all the forcing is provided by the Ekman layer.

This case appears to be most easy to analyse theoretically, to set up experimentally, and to understand intuitively. The experimental system was thus chosen with such an ideal system in mind.

The consequence of the analysis just outlined is however that this seemingly simple system is not simple at all. In fact from the estimates (2.10) and (2.1) we conclude that even *a second order (say $0(E^{1/2})$) divergence of the buoyancy layers will force a zonal flow of the same strength as the one forced by the Ekman layer.* In practice this means that we will always have an error 0(1) with any real apparatus as long as we try to suppress the internal forcing relative to the Ekman layer forcing.

This difficulty may be avoided by accepting the interior meridional circulation as the primary forcing agent and design the apparatus accordingly.

Although such an approach appears logically correct it also has certain drawbacks. As discussed above, the momentum balance becomes degenerate producing a rather special velocity structure. This might be interesting as such but probably less suitable if we want to study the stability of the resulting zonal motion.

Furthermore, we have a free choice of the vertical distribution of the interior forcing and it is hard to decide which particular distribution is the more fundamental. For the moment we have not found it possible to decide upon what path to follow in a future experiment. Hopefully the difficulties outlined above may be avoided on following some basically different line of development.

Let us now discuss under what conditions our basic assumption

$$\frac{\partial \varrho^I}{\partial r} < \frac{\partial \varrho^I}{\partial z}$$

is valid.

In the flow regime under consideration the radial and vertical momentum balance will be close to geostrophic and hydrostatic, respectively. This implies at least the approximate validity of the thermal wind equation; i.e.

$$\varrho_0 2\Omega \frac{\partial v^I}{\partial z} = -g\frac{\partial \varrho^I}{\partial r} \tag{2.14}$$

or

$$\frac{\partial \varrho^I}{\partial r} \Big/ \frac{\partial \varrho^I}{\partial z} \sim \varrho_0 \frac{2\Omega v^I}{g\,\Delta\varrho}$$

where $\Delta\varrho$ is the externally imposed density difference which determines the strength of the basic stratification $\varrho^I(z)$.

Taking now the estimate for v^I given by (2.11) we obtain

$$\frac{\partial \varrho^I}{\partial r} \Big/ \frac{\partial \varrho^I}{\partial z} \sim sH\frac{\varkappa}{\nu}\left(\frac{2\Omega}{N}\right)^2 \tag{2.15}$$

where N is the stability frequency defined by

$$N^2 = \frac{\Delta\varrho}{\varrho_0}\frac{g}{H}$$

If instead we take the estimate for v^I as given by (2.9) we obtain

$$\frac{\partial \varrho^I}{\partial r} \Big/ \frac{\partial \varrho^I}{\partial z} \sim sH\frac{\varkappa}{\nu}\left(\frac{2\Omega}{N}\right)^2 E^{1/2} \tag{2.16}$$

From (2.15) and (2.16) we find naturally that the slope of the isotherms depend on the strength of the forcing as given by sH and on the type of forcing as shown by the difference between (2.15) and (2.16). We can also see that the isotherm slope can always be made small by choosing a sufficiently large stability frequency.

Some special calculations

In the region R_1^I (see Fig. 1) we have according to the analyses in I

$$\varrho^I(z) = \frac{\oint s\hat{\varrho}\, dl}{\oint s\, dl} \tag{2.17}$$

where dl represents a line integral around all sides of the surface obtained when cutting through the container at a level surface z. In our experiment the region is an annulus with inner and outer radii r_2 and r_1, $\hat{\varrho}$ takes on the value ϱ_2 on the inner wall of thickness d_2, and ϱ_1 on the outer wall of thickness d_1.

Recalling (see I) that

$$s = \hat{k}/kd$$

where $\hat{k}$ and k are the heat conductivity of the wall and the fluid respectively and d is the thickness of the wall. Applying (2.17) to our system we thus find

$$\varrho^I(z) = \frac{\varrho_1 d_2 r_1 + \varrho_2 d_1 r_2}{d_2 r_1 + d_1 r_2} \tag{2.18}$$

We note here that ϱ_1 and ϱ_2 are both independent of z. If consideration is given to the simplest case where $(r_1 - r_2) \ll 1/2(r_1 + r_2)$ and thus, effects of curvature are negligible, equation (2.18) becomes

$$\varrho^I(z) = \frac{\varrho_1 + \varrho_2}{2} + \frac{az}{2\bar{d}}(\varrho_1 - \varrho_2) \tag{2.19 a}$$

and thus

$$\frac{\partial \varrho^I}{\partial z} = \frac{a}{2\bar{d}}(\varrho_1 - \varrho_2) \tag{2.19 b}$$

where we have used the following expression for d_1 and d_2

$$\left.\begin{array}{l} d_1 = \bar{d} - az \\ d_2 = \bar{d} + az \end{array}\right\} -\frac{H}{2} \leqslant z \leqslant \frac{H}{2} \tag{2.20}$$

Making use of (2.19) and the expression for m^B as given by (2.3) we obtain

$$m^B = \varkappa \frac{\hat{k}}{ka} \tag{2.21}$$

We thus find that within the narrow gap approximation the interior density field is linear and the boundary layer non-divergent in the region R_1^I.

It is also clear from (2.19) and (2.21) that the stratification and the boundary layer flux may be chosen independently, as pointed out in the previous sub-sections.

Since m^B is essentially a measure of the degree of forcing of the system (such quantities as zonal flow, slope of isotherms etc., are roughly proportional to m^B), this means that we may at least in principle start with a stratified, rotating, stagnant system and successively increase the forcing until the system becomes unstable. In practice this of course requires change of the boundary conditions with considerable practical complications.

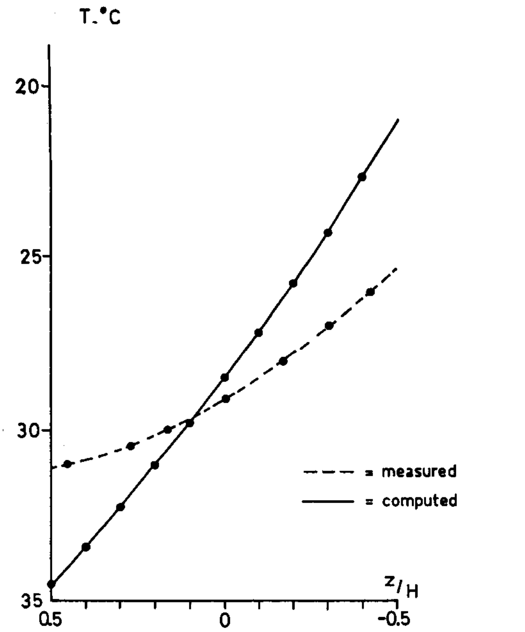

Fig. 2. Measured and computed depth/density plots for nominally correct values of $\bar{d}$ and a (3.8 mm and 0.04 respectively) for case of $\varrho_1 \equiv 39.6$°C, $\varrho_2 \equiv 15.2$°C.

In the present laboratory experiment, it is not justifiable to ignore entirely the effects of curvature. From (2.18) and (2.20) we find

$$\varrho^I(z) = \frac{\bar{d}(\varrho_1 r_1 + \varrho_2 r_2) + az(\varrho_1 r_1 - \varrho_2 r_2)}{\bar{d}(r_1 + r_2) + az(r_1 - r_2)} \tag{2.22}$$

Taking data for a given non-rotating experiment, and substituting into (2.22) all the values appropriate to that experiment, it is possible to obtain a comparison of theoretical and measured profiles. Computed density/depth curves are shown in Fig. 2, together with the measured curve, for the case $\varrho_1 \equiv T_1 = 39.6$°C, $\varrho_2 = 15.2$°C. In the case where nominally correct values of $\bar{d}$ and a are used there is a noticeable quantitative discrepancy between the curves, though the form of the curves are similar.

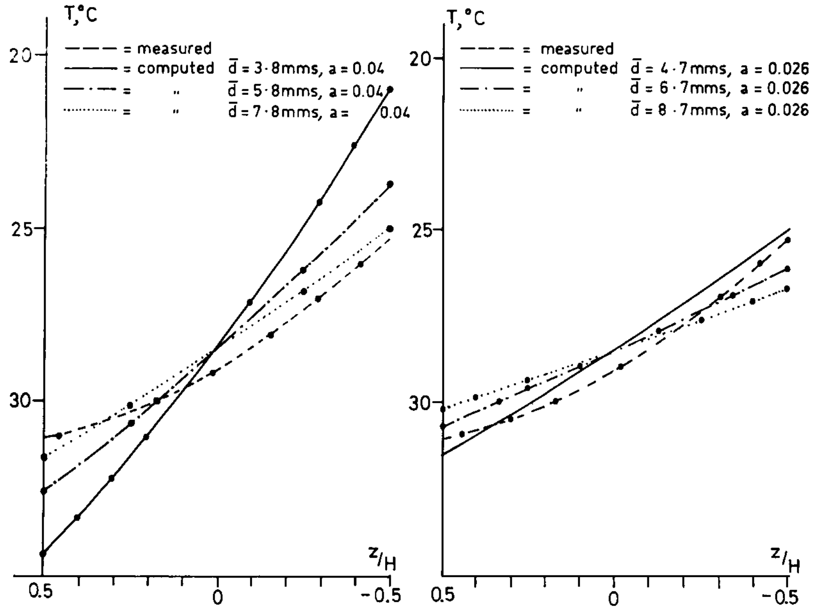

Fig. 3. Comparison of measured depth/density profile with profiles computed for varying $\bar{d}$ and a.

Consideration of the effect of small uncertainties in $\bar{d}$ and a (and to a lesser extent in $(\varrho_1 - \varrho_2)$) reveals that such a discrepancy is more than likely to occur. Graphs showing the effects of changes in $\bar{d}$ and/or a are shown in Fig. 3. It is clear from these graphs that the basic stratification is sensitive to small changes in the values of $\bar{d}$ and a.

There are obvious uncertainties in both these quantities, due to machining difficulties for example ($\bar{d}$ and a are typically 3 mm and $2\,{}^1/_2{}^\circ$ respectively) and the tendency of plexiglass to distort when exposed to heat. Furthermore, uncertainties are produced by the presence of thin thermal boundary layers on the outside of the walls facing the constant temperature reservoirs, which have the effect of artificially adjusting the real $\bar{d}$ and a. Inspection of the sets of curves shows that the measured profile is in satisfactory agreement with theoretical prediction when reasonable variations in $\bar{d}$ and a are taken into account. Variations in ϱ_1 and ϱ_2 also have some influence. Indeed the disparity between the measured and computed values of $\varrho^I(z=0)$ indicates an error in $(\varrho_1 - \varrho_2)$ of about 1°C which is of the same order as errors expected due to temperature fluctuations and other random errors.

One of our main experimental observables was the slope of the isotherms. It is thus of interest to compare such observations with theoretical expectations as given by (2.15) or (2.16). Since our apparatus was constructed such that the forcing through the Ekman layers should dominate we will base our comparison on this case, remembering all the difficulties outlined in the previous sub-section.

Rather than using (2.15) (which describes this case) we will however derive a corresponding expression making use of some of the explicit results valid for our specific geometry.

From the thermal wind equation (2.14) we obtain

$$\theta \simeq \varrho_0 \frac{2\Omega}{gH} \cdot \frac{V_E^I \cdot 2}{(\partial \varrho^I / \partial z)}$$

where θ is the isotherm slope and V_E^I the zonal velocity required by the Ekman layer transport. ($\partial v^I/\partial z$ has been estimated as $2V_E^I/H$ since v^I varies between $\pm V_E^I$ over the height H.) We now take v_E^I from (2.8b), (2.6) and (2.21) and $\partial \varrho^I / \partial z$ from (2.19b). We thus obtain

$$\theta = \left(\frac{16\,\bar{d}\hat{k}}{gHa^2}\right) D \qquad (.23)$$

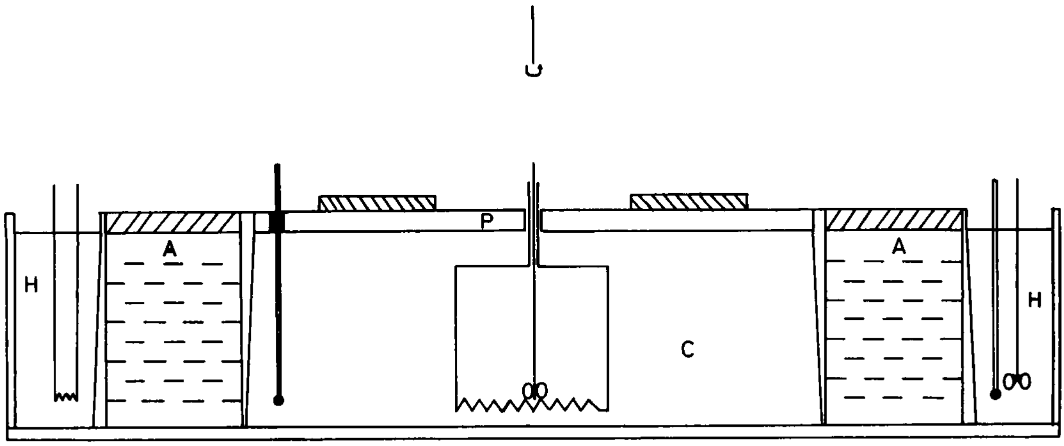

Fig. 4. Schematic view of experimental apparatus.

where

$$D = \frac{\varkappa \Omega^{3/2} \nu^{-1/2}}{k\alpha(\Delta T)}$$

Note that the parameter D contains all the quantities that can be varied using one and the same apparatus. One of the main goals of the experiment has been to obtain measurements to compare with this relationship.

3. Apparatus

A schematic diagram of the experimental apparatus is shown in Fig. 4. The working fluid is contained in a chamber, A, constructed of plexiglass. As shown in Fig. 4 the thickness of the chamber wall facing the hot temperature bath, H, decreases with height and that of the wall facing the cold water bath, C, increases with height. The mean thickness of the wall and the rate of change in thickness with height are the same for both walls, having the values of 3.8 mm and 0.04 respectively. The radii of the inner and outer cylinders forming the annulus are 15.0 cm and 22.5 cm respectively and the height of the fluid region is 10.0 cm. A closed heating bath, H, also constructed of plexiglass, surrounds the annulus and is filled with water. A 500 watt shielded electrical heating coil connected to a thermostat control is immersed in this water which is vigorously circulated round the heating bath by several pumps.

The inner wall of the annulus is cooled by bath C, which is filled with a water/alcohol mixture and covered by a metal plate, P, on which is mounted an array of Peltier elements. An electrically insulated heating strip connected to a sensitive thermistor switch is also submerged in C, and a pump vigorously circulates the cooling liquid. The upper surface of the working fluid chamber is closed by a transparent rigid lid constructed of plexiglass in 3 sections with gaps of 3–4 mm left between the sections. This allows probes to be lowered into the fluid and to be moved radially across the annulus. A thin layer of oil covers the lid to inhibit the troublesome problem of evaporation of the working fluid.

As indicated in Fig. 4 the whole experimental apparatus is mounted on a rotating turntable, the angular velocity of which is monitored by an electronic timer activated by a magnetic switch. The rotating table is equipped with low-noise electrical slip rings and, in addition, coolant water for the Peltier elements can be circulated from the laboratory supply via fluid slip rings in the table axle.

The temperature field in the annulus is determined with a thermistor bead mounted at the tip of a hyperdermic which can be moved vertically and radially by means of a motor and rack and pinion arrangement. The thermistor forms one arm of a Wheatstone bridge circuit and the off-balance voltage is displayed on a digital voltmeter (DVM). A potentiometer is also attached to the rack and pinion assembly

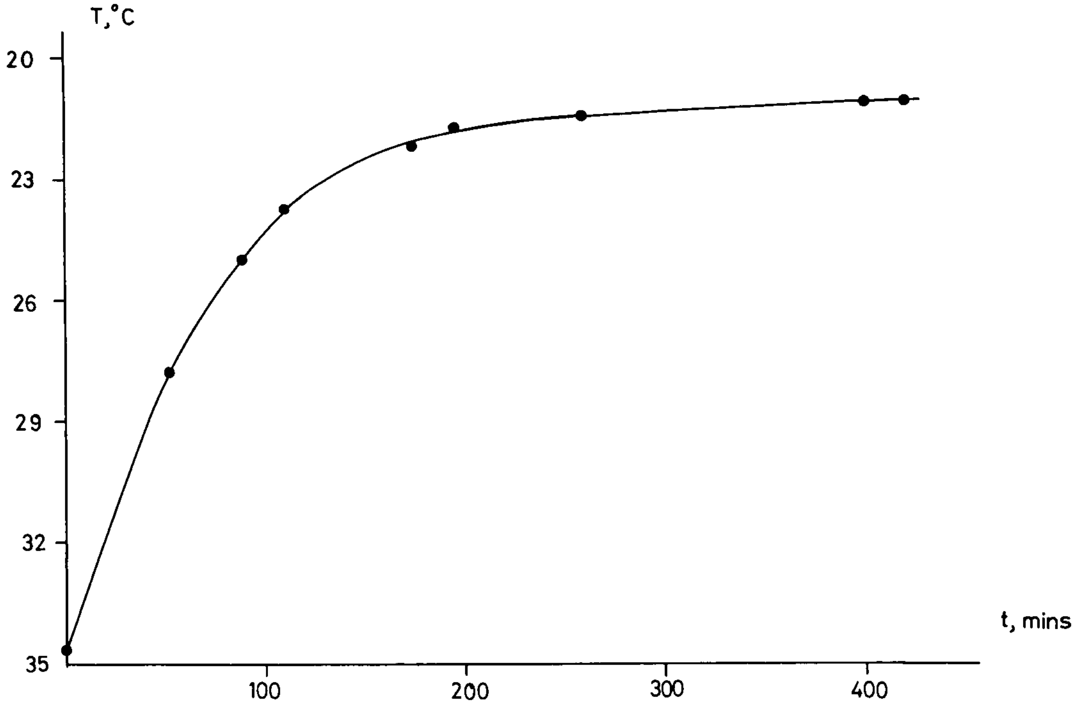

Fig. 5. Temperature/time output from fixed thermistor situated in the annulus (non-rotating), having horizontal temperature difference of 20°C.

to indicate the vertical position of the thermistor bead. This enables temperature and depth measurements to be obtained simultaneously.

The pH technique developed by Baker (1966) is used to measure flow velocities in the fluid, the dye being released from a taut horizontal wire stretched between two rigid vertical supports. The chemical indicator used is thymol blue and the dye-releasing D.C. voltage is applied between the wire and one of the supports. Another rack and pinion arrangement allows the dye wire to be raised or lowered, enabling horizontal velocity profiles to be obtained at any depth in the fluid. A 35 mm 'Robot' camera mounted above the annulus, on a frame bolted to the turntable, records the dye patterns produced.

4. Experimental results

4.1. *Adjustment time*

Before conducting experiments with the annulus in motion, several investigations were made into the non-rotating case in order to develop certain measuring techniques and to make some checks with theoretical prediction.

It was shown in I that for the non-rotating case, under the conditions of the present experiment, the adjustment time of the fluid to steady state is much less than the diffusion time. Specifically, the adjustment time, τ, is estimated to be

$$\tau \sim \min\,(L^2/\varkappa,\ L^2/\varkappa s L)$$

if

$$H/L \sim 0(1)$$

and thus, if $sL \gg 1$, τ is much less than the diffusion time, $L^2/\varkappa$.

An experiment was performed in which a stable stratification was set up in the annulus, using the method described in *I* and the apparatus was then left overnight to ensure that a steady state had been attained. The thermistor sensor was situated at a fixed position in the interior of the fluid region. The stable stratification was then disturbed by impulsively starting and stopping the rotating table, causing strong mixing to occur throughout the fluid interior. The time taken for the fluid to re-establish the original state (the adjustment time) was then determined by recording the thermistor signal as a function of time. The results of this experiment are shown in Fig. 5. It is seen how, after cessation of the imposed agitation at $t=0$, the temperature at a fixed point in the fluid interior approaches an asymptotic value almost exponentially. The adjustment time, taken as the e-folding time calculated from Fig. 5 is estimated to be approximately 100 min. Inserting the values appropriate for the experiment, $L=7.25$ cm, $\varkappa = 1.4\times10^{-3}$ cm^2 sec^{-1}, $k=2.1\times10^{-3}$ watt cm^{-2} (°C/cm)$^{-1}$, $k\sim5.9\times10^{-3}$ watt cm^{-2} (°C/cm)$^{-1}$, $\bar{d}=0.45$, into the expression above it is seen that the calculated adjustment time agrees very satisfactorily with the experimental determination. Less comprehensive measurements of the adjustment time were taken with the system rotating. In these cases the output of the temperature sensor situated at a fixed depth in the fluid was monitored on a chart recorder as the rotation rate of the apparatus was changed. The effect of the change in rotation rate was clearly seen on the trace and the time taken for the temperature at the reference level to re-establish its previous value could be estimated. Such preliminary measurements indicated a much shorter adjustment time than in the non-rotating case (by a factor of about 50 for the case of a horizontal temperature difference of 25°C, for example).

4.2. *Velocity measurements in the rotating annulus*

Using the pH technique described earlier, horizontal velocity profiles were recorded photographically at various depths in the fluid interior. In this way it was possible to estimate not only the order of magnitude of the interior flows but also the vertical shear of the horizontal velocity. Successive lines of dye—usually 4 or 5—were produced at a given level by pulsing the wire at known time intervals, and the subsequent development of these dye lines was studied. By measuring the angular displacements of the lines in the known time intervals an average azimuthal velocity could be estimated for that particular level: furthermore, by studying the patterns at different levels the vertical shear could be estimated.

Measurements from the above figures indicate an average azimuthal velocity of about 0.5 mm/sec at a level just above the Ekman boundary layer on the rigid bottom surface of the annulus, and a vertical shear of $\sim10^{-2}$ sec^{-1}. (The azimuthal velocity at a given depth is clearly dependent also upon radius and it is noted that the values obtained above are from measurements of maximum velocity points on the profiles.)

These estimates are in satisfactory agreement with other indirect experimental evidence from measurements in the wave regime (see next section) and with theoretical expectations. The latter can be demonstrated by substituting the appropriate values for $\varkappa$, a, k/k and ν (1.4×10^{-3} cm^2 sec^{-1}, 0.04, 0.36, and 10^{-2} cm^2 sec^{-1}, respectively) into the order of magnitude expression (2.11), together with the relevant value of the rotation rate.

4.3. *Wave regime*

One of the basic aims of the investigation was to determine whether, and under what conditions, the basic flow in the rotating annulus became unstable. In this section the various techniques used to detect any transitions from the so-called symmetric regime to the regular wave regime are explained and the main results obtained through use of such techniques are described.

The most sensitive means of detecting any transition was to record continuously the signal from the thermistor sensor as the various external parameters were changed. In these experiments the imposed horizontal temperature gradient was kept fixed throughout by presetting the hot and cold bath thermostats, and changes in the interior flow were caused only by increasing the rotation rate of the annulus. The procedure followed after pre-setting the thermostats was to lower the thermistor to a given position in the fluid interior and to set the table rotating at a given rate, leaving it for several hours to establish a steady state. The thermistor bead was fixed in the middle of the annulus at a depth position of about $-0.3H$ (H being the total depth of the fluid) and the thermistor remained fixed at this position throughout the experiment. When the fluid was judged to have reached a steady state the signal from the thermistor was recorded on a pen recorder for a period of 1–2 hours. The rotation

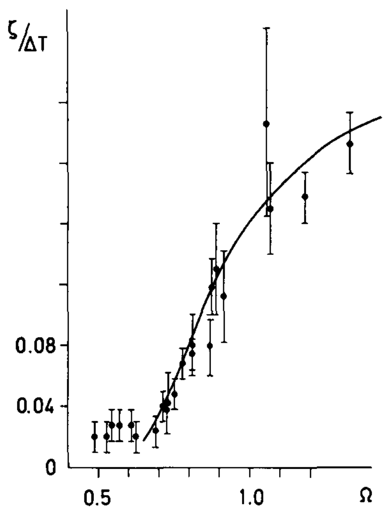

Fig. 6. Plot of non-dimensional wave amplitude, $\zeta/\Delta T$ against Ω for $\Delta T = 19.0°C$, at $Z/H = -0.3$.

rate was then slightly increased ($\sim 5\%$) and the signal recorded again for 1–2 hours. This procedure was repeated several times until the temperature trace showed a steady system of waves. A series of traces were then taken, as above, with the rotation rate being changed up or down to scan the transition region and also, to a lesser extent, to study the development of the waves as the rotation rate was further increased.

Most of the stability experiments were performed with water as the working fluid. However, additional measurements using glycerine and glycerine/water mixtures were also made, as shown later.

The appearance of waves was clearly indicated on the traces, though, as expected with a non-continuous increase or decrease in rotation rate, it was not possible to identify directly if a critical value of Ω above which the waves occur existed, and if so what was its value. An interesting feature of the traces, however, was that, having reached the wave regime, the amplitudes of the temperature fluctuations showed a steady increase with increasing Ω. This effect, which was found to be common to all such experiments, gave rise to a useful method of estimating a critical value of Ω (Ω_{crit}, say). A typical plot of wave amplitude, ζ, against rotation rate, Ω, is shown on Fig. 6. The values of ζ, which are average values (obtained from measurements of several cycles on a particular temperature/time trace) have been normalised by ΔT—the horizontal temperature difference imposed between the outer walls of

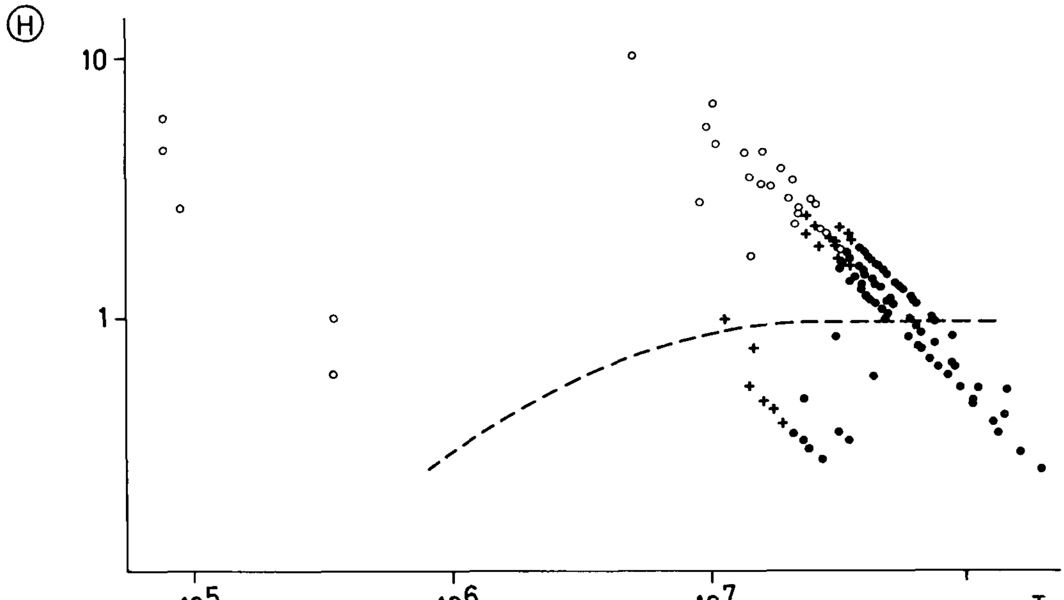

Fig. 7. Plot of Θ against Ta showing comparison of data points obtained (● = waves present, ○ = no waves detectable, + = presence of waves uncertain) with stability curve --- of Kaiser (1970).

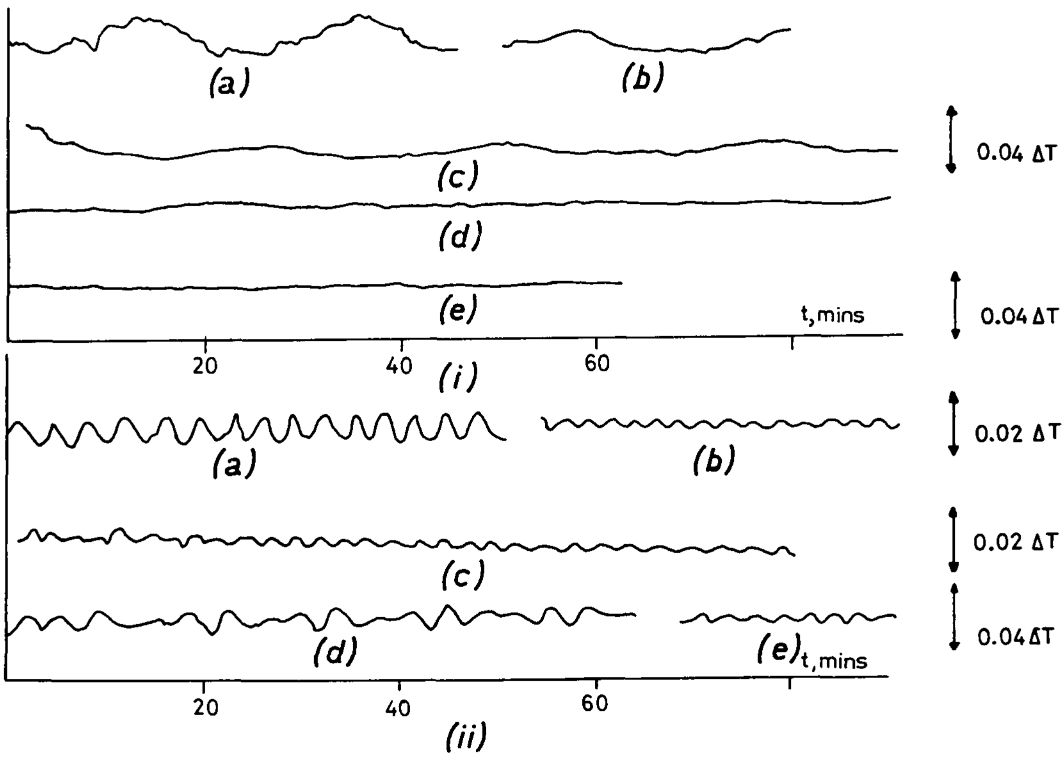

Fig. 8. Temperature/time output from a thermistor fixed in the fluid at a level $Z/H = -0.3$ for (i) rigid lid and (ii) free surface cases. $\Delta T = 15.0°C$ in both cases. Rotation periods (i) are (*a*) 4.9 sec, (*b*) 8.4 sec, (*c*) 9.8 sec, (*d*) 10.6 sec, (*e*) 12.0 sec. Rotation periods (ii) are (*a*) 8.0 sec, (*b*) 9.8 sec, (*c*) 10.8 sec, (*d*) 11.6 sec, (*e*) 13.1 sec.

the annulus. Uncertainty limits on ζ are also obtained by measuring the variation in wave amplitude from cycle to cycle on a given trace —for a recording time interval of a few hours a typical trace would contain between 5 and 10 complete cycles. Estimates of Ω_{crit} can be obtained from figures such as Fig. 6 though, clearly, these estimates are subject to errors of the order of 15%.

The total data from the experiments are shown in slightly different form on Fig. 7 together with the relevant portion of the stability curve obtained by Kaiser (1970) and others. The two non-dimensional parameters Θ and Ta (thermal Rossby number and Taylor number respectively) are defined as

$$\Theta = \frac{g\alpha H(\Delta T)}{\Omega^2 L^2}$$

$$Ta = \frac{4\,\Omega^2 L^5}{\nu^2 H}$$

where α and ν, both of which are temperature dependent quantities, are average values over the temperature range of the experiment and ΔT is the horizontal temperature difference applied to the outer walls of the annulus. To avoid confusion, data points for estimated values of Ω_{crit}, obtained from figures such as Fig. 6 are not plotted.

The restricted range of the present experiments is seen from Fig. 7. In order to construct a comprehensive stability curve for this type of annulus and then to make detailed comparison with earlier investigations (Kaiser, 1970; Fowlis & Hide, 1965) it is clear that much more data would be required. (Indeed, as we state earlier and stress again here, such a comparison has not been the aim of these experiments.) However, an obvious feature of the graph is that, for a given value of Ta, the values of critical Θ are significantly higher than the "classical" annulus case, as exemplified by Kaiser's results. This may be a real effect partly

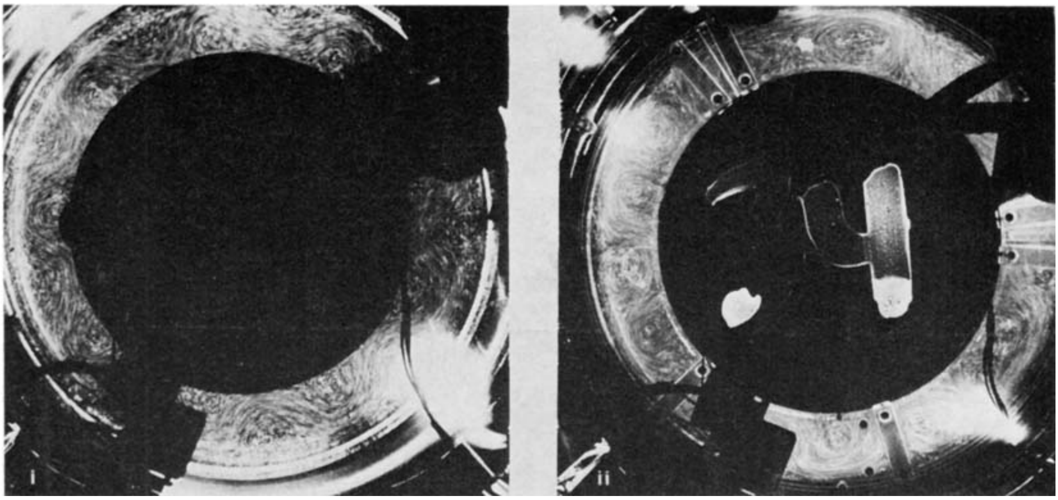

Fig. 9. Plan photographs showing wave motions at mid-depth in the annulus for (i) free surface and (ii) rigid lid cases for $\Delta T = 20°C$. Data for (i) $\Omega = 0.86$ rads/sec, exposure time 3 sec (ii) $\Omega = 1.13$ rads/sec exposure time 25 sec. Note that the patterns are not surface patterns and that the lengths of the streaks in both photographs are about the same, though the exposure times differ greatly.

due (Fein, 1973) to the different upper boundary conditions in the 2 investigations, though much of this discrepancy can be explained by the value of ΔT used in the definition of Θ. In contrast to the case of the copper or brass annulus, such as the one used by Kaiser, there is clearly a substantial temperature drop through the plexiglass walls and thus the inner wall temperature difference (the temperature difference the fluid actually 'feels') will be less than ΔT. Basing the thermal Rossby number on an *inner* wall temperature difference, therefore, is consistent with a shift of the data towards the stability curve shown.

Experiments were also run with the rigid lid removed to determine the free surface stability of the flow. Temperature trace data from such experiments served to demonstrate the increase in frequency of the waves in going from a rigid lid to a free surface upper boundary, for otherwise identical conditions, as shown on Fig. 8. In addition, it was observed that, for a given ΔT, the wave instability appeared earlier (i.e. at a lower Ω_{crit}) than in the rigid lid case. This difference in behaviour between the two cases is shown in Fig. 8.

In order to ehck that the temperature oscillations observed on the pen recorder traces were actually due to the presence of baroclinic waves in the annulus, the flow was visualised using a technique developed by Douglas et al. (1972). Small (~ 0.5 mm diameter) polystyrene beads were mixed with the fluid and a narrow, horizontal collimated beam of light illuminated a thin region at a given depth in the annulus. The density of the working liquid was first of all increased slightly (by addition of a small quantity of glycerine) in order that the polystyrene particles (density 1.05 gm/cc) should be neutrally buoyant and thus remain in permanent suspension. The motions occurring at the illuminated level were then recorded by taking time exposures with the camera mounted above the apparatus. An advantage of this technique is that the flow can be observed at any chosen depth in the fluid merely by raising or lowering the collimated beam: this avoids the restriction of having to consider surface flow patterns which are not necessarily typical of the flows occuring in the interior regions.

The thermistor sensor, connected to the pen recorder, was also lowered to the same depth in the fluid as the illuminated region and flow patterns were recorded with both free surface and rigid lid upper boundaries. Following the same procedure as before, the rotation rate was incrementally increased, for a pre-set ΔT, and simultaneous flow patterns and temperature traces were recorded. In both cases it was confirmed that, indeed, the onset of the tempera-

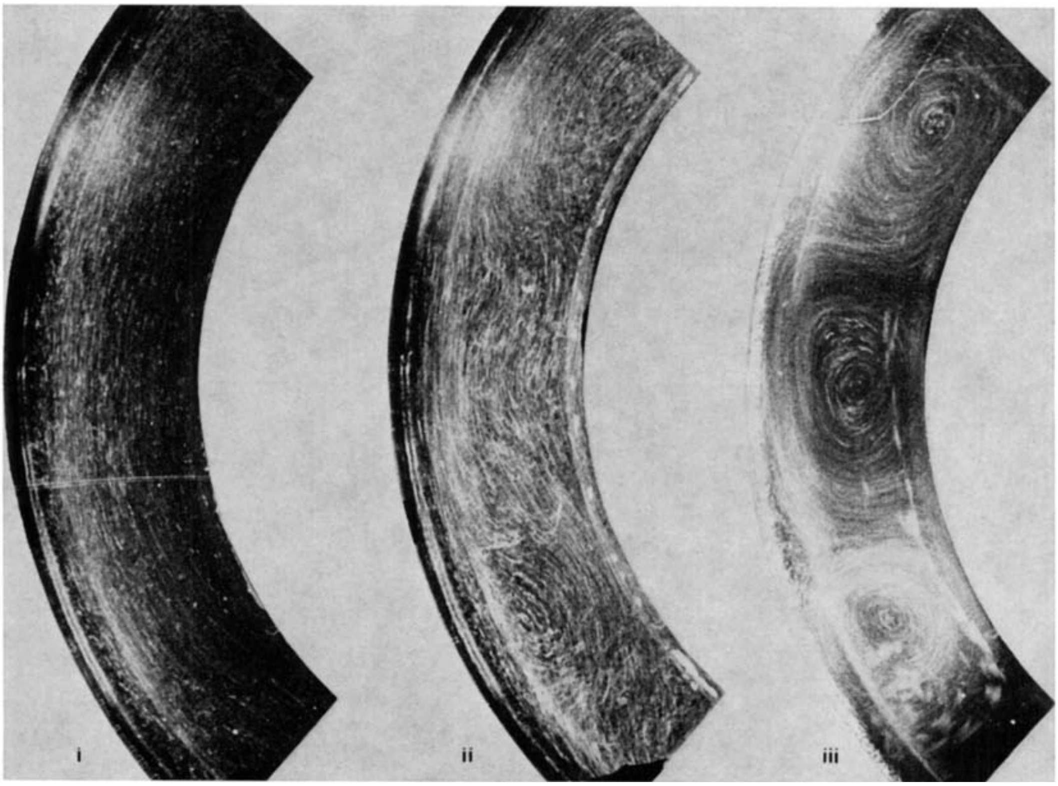

Fig. 10. Plan photographs showing the transition to the wave regime for the rigid lid case. All photographs are taken at the same depth in the fluid with an exposure time of 30 sec. The value of $\Delta T = 20°C$ and $\Omega =$ (i) 0.49 rads/sec, (ii) 0.58 rads/sec, (iii) 0.79 rads/sec, and (iv) 1.91 rads/sec.

ture oscillations corresponded to the occurrence of wave motions in the annulus. Particularly with a free surface the correlation could be seen directly by eye, the wave motions and associated vortices being so vigorous and well-defined. However, with a rigid lid in position the average velocities in the fluid were much reduced due to the formation and frictional effect of an Ekman boundary layer at the top. In this case it was necessary to record the patterns with time exposures of about 20–30 sec in order to see the baroclinic waves, and no eye-check was possible.

Photographs taken in the wave regime are shown on Fig. 9. It was established from such figures that throughout the depth of the fluid a steady system of waves occurs in a particular parameter regime and that this system of waves drifts slowly around the annulus.

The baroclinic waves observed with a free upper boundary are essentially identical to those observed in other related annulus studies. The presence of the steady wave system with a well developed jet stream transporting heat from the hot to the cold walls and an alternating system of vortices are well demonstrated in Fig. 9. In the rigid lid case the flow pattern is clearly not so well defined, though the occurrence of waves is observed. The jet-stream, though apparent, is not so well developed and in some areas the pattern resembles more a system of closed cellular vortices. It is possible that this absence of regularity was due to the wave pattern being locally distorted by the heating or cooling not being azimuthally symmetrical. Photographs are shown in Fig. 10, for the rigid lid case, in which the various stages in going from symmetric to wave regime are demonstrated.

A slightly more easy and versatile (though less comprehensive) method of detecting the presence of waves in the annulus was to em-

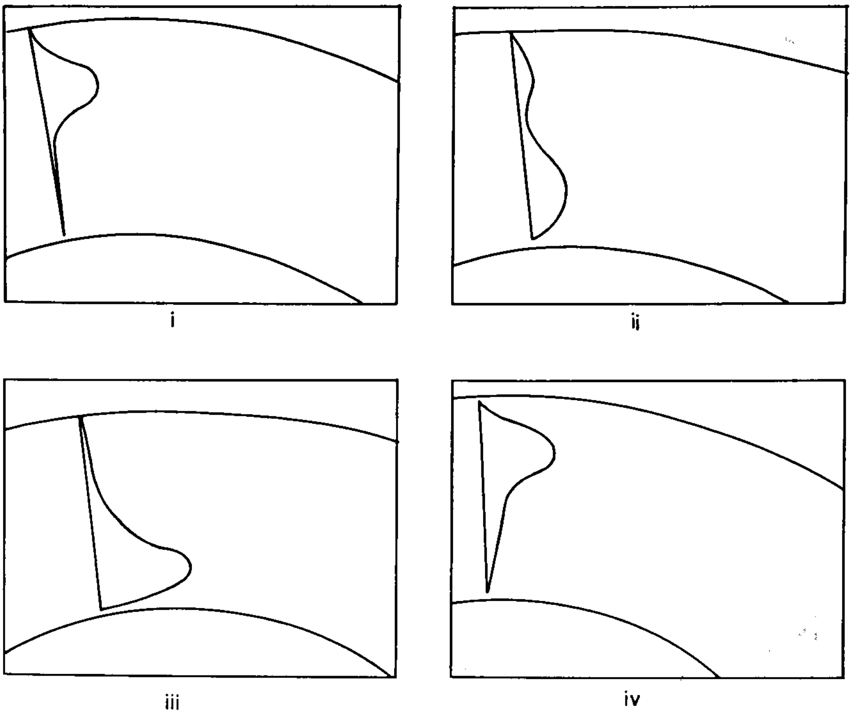

Fig. 11. Motion of horizontal dye lines produced at times (i) $t = t_0$, (ii) $t = t_0 + 2$ min, (iii) $t = t_0 + 4$ min and (iv) $t = t_0 + 7$ min, showing presence of waves in the annulus at a level $z/H = -0.04$. Sense of Ω is anticlockwise.

ploy the pH-technique described earlier. With this method a line of dye was produced at a given depth in the fluid and the distortion to the dye profile caused by the passage of the wave was recorded. The time development of a dye line profile illustrating the complete cycle is shown for a particular level on Fig. 11.

4.4. *Temperature measurements: nonrotating*

In an extensive series of experiments the temperature field in the interior of the fluid has been determined over a wide range of conditions. Temperatures have been measured with the movable thermistor arrangement and, from these measurements, isotherm fields have been plotted.

Experiments were first of all conducted using water as the working fluid and with the annulus non-rotating. (Note that all temperature measurements to be described were obtained with a rigid lid upper boundary condition.) Using the DVM, temperature/depth readings were taken at 10–12 radial stations in the annulus interior, together with 3–4 soundings in both side-wall boundary layers. At a particular radial station the temperature versus depth plot was obtained by lowering the thermistor vertically in a series of small steps (usually 15–20) and recording the measurement at each level. By repeating this procedure for each station the whole fluid cross section could be scanned and interior temperatures could be obtained at 200–250 "grid points". On lowering the thermistor from one level to the next it was necessary to wait 1–2 minutes before the DVM reading became steady—the time delay being caused by the response time of the thermistor and possibly by the disturbing effect of the probe on the ambient fluid (Fultz & Kaiser, 1972). On completion of a scan across the annulus, less comprehensive repeat soundings were taken at alternate radial stations (in quasi-random order) to check the reproducibility of the data.

From such temperature/depth soundings the isotherm field in the annulus interior could be

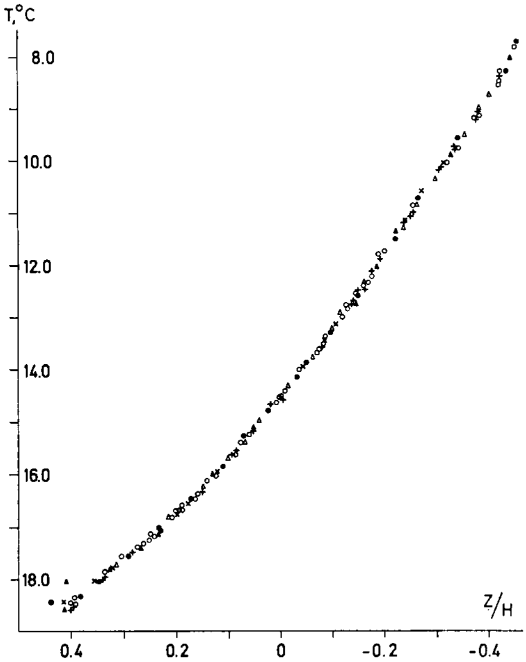

Fig. 12. Compound plot of temperature against depth for 12 radial stations in the non-rotating annulus having $T_1 = 38.9°C$, $T_2 = 15.2°C$.

constructed, as shown on Fig. 14 (i). Several such constructions were made for varying values of ΔT, and, to a lesser extent, for different fluids (water, glycerine and water/glycerine mixtures). The errors in each grid point in Fig. 14 are not indicated but it was clear that they were sufficiently large to make any marked kinks in the isotherms insignificant. The main feature of Fig. 14 (i) is the good agreement with the theoretically predicted very small slope of the isotherms. Inspection of the data showed the agreement to be better in cases where the working fluid was less viscous and where ΔT was large—as expected from a theory in which the momentum balance in the main part of the region is dominated by the buoyancy force. Fig. 12 shows a compound plot of all data from all radial stations in order to illustrate the flatness of the isotherms: it is observed that there is no systematic increase or decrease in temperature along a given depth contour.

4.5. *Temperature measurements in the rotating annulus*

In obtaining temperature fields with the rotating annulus the same procedure as above

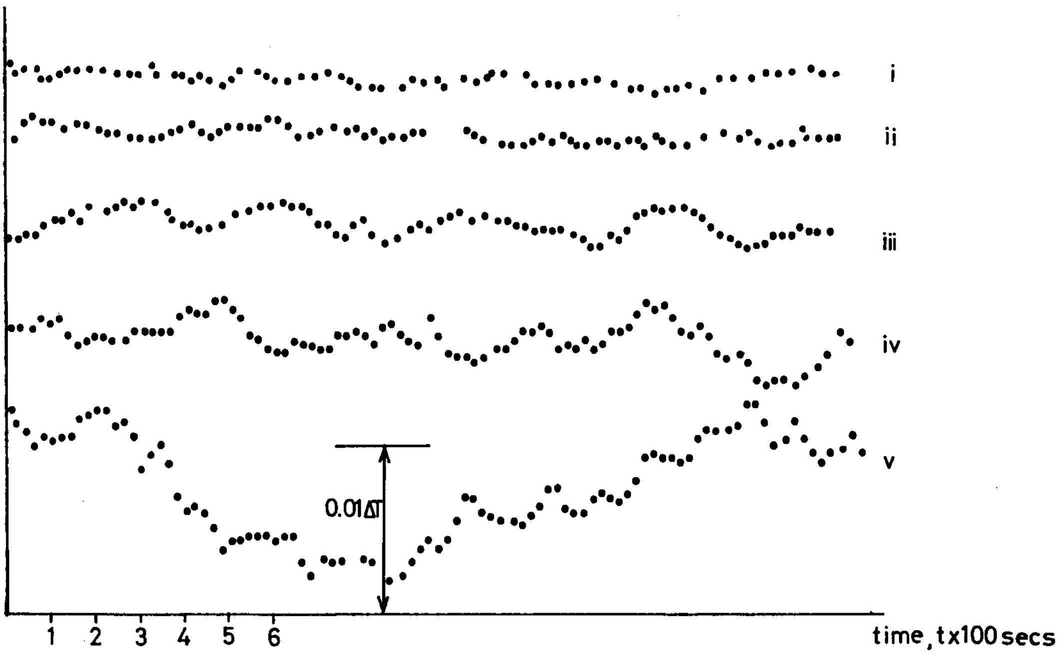

Fig. 13. Temperature/time output from a thermistor fixed at $z/H = -0.3$, recorded from the DVM for the rotating annulus with a rigid lid and $\Delta T = 20°C$ in the cases (i) $\Omega = 0.39$ rad/sec, (ii) $\Omega = 0.53$ rad/sec, (iii) $\Omega = 0.54$ rad/sec, (iv) $\Omega = 0.69$ rad/sec, (v) $\Omega = 0.80$ rad/sec.

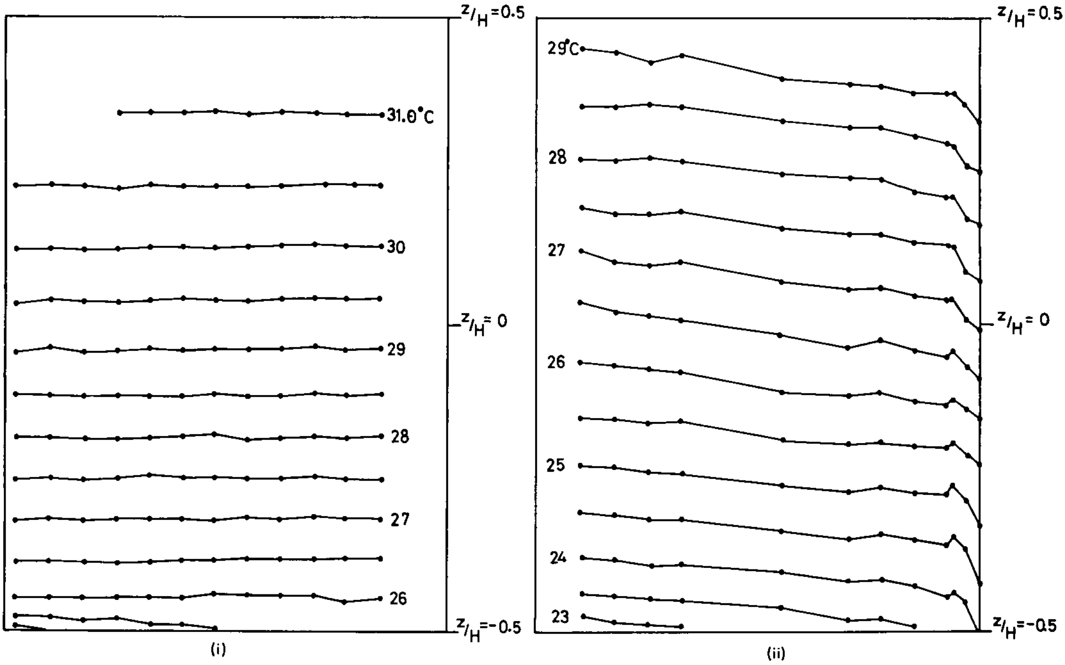

Fig. 14. Temperature field in (i) the non-rotating and (ii) the rotating annulus showing 0.5°C isotherms for the cases, (i) $T_1 = 38.9°C$ $T_2 = 15.2°C$, $\Omega = 0$, (ii) $T_1 = 33.8°C$, $T_2 = 15.6°C$, $\Omega = 0.52$ rad/sec.

was followed, usually using water as the working fluid and making use of various combinations of Ω and ΔT. Most of the data was collected in the symmetric flow regime though some later measurements were obtained with fully developed wave motions present in the annulus. In the former circumstance a temperature/time trace was taken at a fixed depth, as before, to ensure no oscillations were present before starting the measurement programme. Where possible, instead of using the pen recorder for the purpose the D.V.M. output from the thermistor was sampled every 10 sec for a period of 20–30 minutes. This method, though tedious, proved very sensitive, as shown by Fig. 13.

Isotherm fields were obtained for about 25 different Ω, ΔT settings in the symmetric regime, one of which is shown in Fig. 14, together with a non-rotating case for comparison. As with the non-rotating case, most attention was focussed on the interior region of the fluid, but in some instances additional information was obtained in the side-wall boundary layers, the lateral extent of which was of the order of $0.1H$ (see Fig. 14). The effect of rotating the annulus is clearly seen; the isotherms begin to slope even at slow rotation speeds and as Ω is increased, keeping ΔT fixed (i.e. as Θ is decreased and Ta

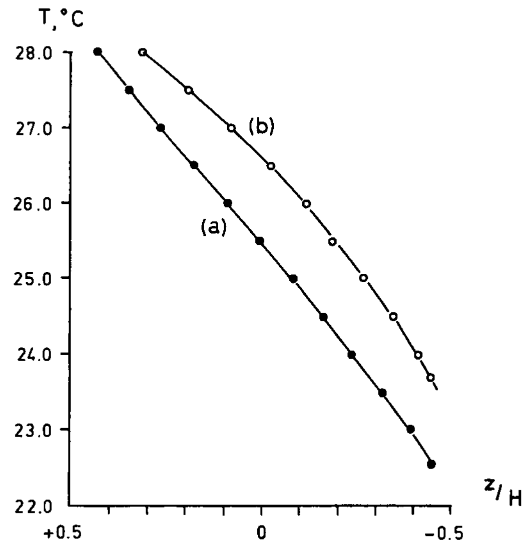

Fig. 15. Temperature/depth plots comparing (*a*) rotating and (*b*) non-rotating cases for $T_1 = 32.4°C$, $T_2 = 15.2°C$. In (*a*), $\Omega = 0.45$ rad/sec.

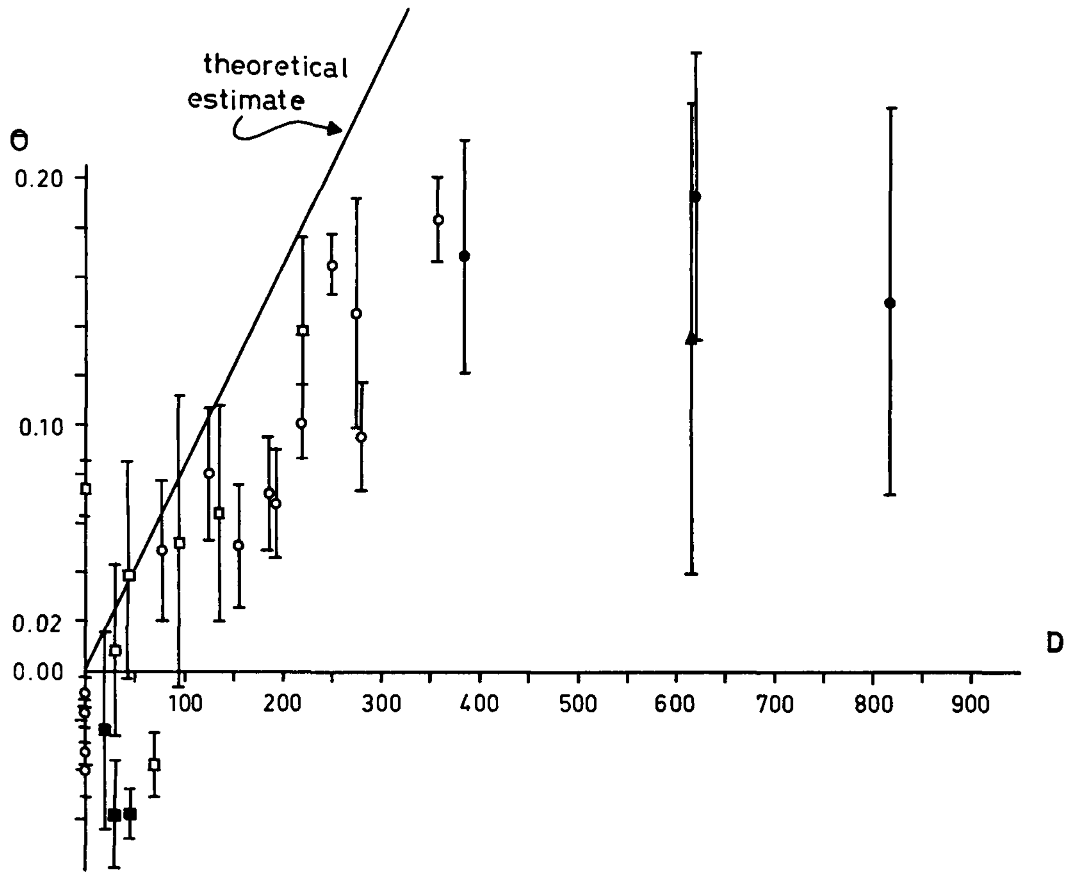

Fig. 16. Plot of experimental data in the form of isotherm slope θ against parameter D together with the theoretical estimate from 2.23. Data points shown are for ○ = water, symmetric regime, ● = water, wave regime, ▲ = 38 % glycerine/water solution, wave regime, □ = 70 % glycerine/water solution, symmetric regime, ■ = glycerine, symmetric regime.

similarly increased) the slope of the isotherms increases also. Characteristic boundary layer behaviour is observed adjacent to both hot and cold walls but in the few cases investigated no noticeable difference in such behaviour is seen in the non-rotating and rotating situations.

Similarly, it is confirmed that the basic stratification in the interior of the fluid remains unaltered by the presence of the rotation. This is demonstrated by Fig. 15 which shows temperature/depth plots for cases with and without rotation but in which all other imposed conditions remain the same. From Fig. 15 it can be seen how the introduction of rotation causes the isotherm to tilt, producing a different temperature at a given depth, whilst the basic stratification, as indicated by the slope of the curves, remains essentially unchanged, as expected.

Using a least squares fit procedure the slopes of the isotherms in the interior region of the fluid were calculated. As expected, for a particular Ω, ΔT combination the isotherm slope varied considerably with depth, even outside the boundary layer regions. For purposes of comparison between different sets of data and, particularly, with theoretical prediction, an average value over the full depth of the interior (defined arbitrarily as being between $+0.35H$ and $-0.45H$) is taken and the standard deviation calculated. In the construction of the isotherm fields the errors for each data point were calculated: however, it was found that the resulting error in a given isotherm slope was less than that represented by the spread of the data over the fluid depth. The uncertainty in the average isotherm slope was thus taken as the standard deviation quantity just described.

In situations where the regular baroclinic waves were present in the annulus, less-detailed measurements of isotherm slope were taken. To obtain an order of magnitude estimate in such cases, time-averaged temperature measurements were made at 4 reference points in the fluid interior. Using the values of $\partial T/\partial z$ and $\partial T/\partial r$ calculated from the above data, the isotherm slope could then be computed. A plot of θ against D is shown on Fig. 16. As stated earlier, the data has been collected with water, glycerine and water/glycerine mixtures as working fluids: this is indicated in the above figure as is the distinction between data points obtained in the symmetric and wave flow regimes.

All the data points plotted are shown with relatively large associated uncertainty limits. For points in the symmetric regime these limits simply represent the large variation in isotherm slope with depth, remarked upon earlier. Similarly, in the wave regime, since the values of θ are obtained from time averages of oscillatory temperature signals, the uncertainty limits shown are indicative of the amplitudes of these oscillations. In particular, in the latter circumstance, a large uncertainty is produced when calculating a horizontal temperature difference since this involves subtracting two quantities which when averaged are almost equal but which both necessarily exhibit large amplitude oscillation with time.

Using appropriate values of the constant quantities $\bar{d}$, g, H and a, and using an average value for the thermal conductivity of plexiglass, the theoretical estimate of the gradient of the θ, D plot, obtained from (2.23) is also drawn in Fig. 16.

In the symmetric flow regime there is an obvious discrepancy between the data and the theoretical estimate though, particularly with water as the working fluid, there is good agreement with the predicted linear behaviour. The discrepancy is not serious, however, remembering that the theoretical line is only an order of magnitude estimate. In addition, and perhaps more significant, D is made up of several quantities ($\varkappa$, k, α, ν) which are strongly temperature dependent, and in computing the data points for D only average values (i.e. for a reference temperature of 15°C) were used. When the variation with temperature is taken into account (for example, for water, the Prandtl number, $\nu/\varkappa$, varies from 8.8 at 15°C to 5.5 at 30°C) the data shows satisfactory agreement with the theoretical estimate. It is of course noticeable that the increase of slope with increasing D takes place only in the symmetric regime. When waves appear in the annulus—apparently when θ is of the order of 0.18—the graph has a different behaviour. More data is obviously required in the wave regime but it seems to be clear that the slopes of the isotherms cease to increase at the same rate with increasing D and indeed there is evidence that the slope drops on crossing the stability boundary. This is consistent with the readjustment of the temperature field expected after such a significant change in the nature of the flow, and the effect is in agreement with that observed by experimentalists working with the "classical" annulus.

5. Summary and conclusions

The results of the experimental investigation have shown encouraging agreement with theoretical prediction in several important respects. Quantitative measurements of the adjustment time of the fluid and the interior temperature structure in the non-rotating case have confirmed earlier theoretical and qualitative results (I) and have shown the applicability of these results to the annulus configuration.

With the annulus rotating it has been shown that regular baroclinic waves occur in the fluid in a certain parameter range though these wave motions have a more well-defined character then the upper surface of the fluid is free. With a rigid lid in position, interior horizontal velocities are significantly reduced and there is a suggestion that the parameter range for the occurrence of waves in the two cases (i.e. free surface, rigid lid) is different.

Good agreement with theory is shown with the isotherm data—the bulk of the investigation. The application of the results in I to a physically realistic *rotating* problem, using an annulus specially constructed with regard to the boundary conditions, has been successful in predicting the basic stratification in the annulus and the dependence of the isotherm slope upon the physical properties of the boundaries and the fluid. The graph of isotherm slope against the parameter D shows an essentially linear relationship in the symmetric regime, while a somewhat different behaviour was indicated in the wave regime. As stated in the previous section, this is a most natural result of the significant change in the character of the flow (and the consequent introduction of a different heat transfer mechanism) causing the observed readjustment in the temperature field. The value of the isotherm slope at the symmetric/wave regime boundary was shown to be of the order of 0.18, indicating that at least one important condition of the Eady theory (Eady, 1949) that the order of the isotherm slope should be much less than unity—is fulfilled in these experiments.

6. Acknowledgements

The authors wish to acknowledge particularly the help of Mr S. Å. Odh who played a major role in the design and construction of the apparatus and who helped in the collection of many of the results. One of the authors (P. A. D.) acknowledges the financial support of both The Royal Society, during the tenure of a post-doctoral fellowship under its European Exchange Programme, and the International Meteorological Institute in Stockholm.

REFERENCES

Douglas, H. A., Hide, R. & Mason, P. J. 1972. An investigation of the structure of baroclinic waves using three-level streak photography. *Quart. J. Roy. Met. Soc. 98*, 247.

Eady, E. T. 1949. Long waves and cyclone waves. *Tellus 1*, 33.

Ekman, V. W. 1905. On the influence of the Earth's rotation on ocean currents. *Arkiv. Matem. Astr. Fysik Stockholm 2* (11), 1.

Fein, J. 1973. An experimental study of the effect of the uppear boundary condition on the thermal convection in a rotating differentially heated cylindrical annulus of water. *Geophys. Fluid. Dyn. 5*, 213.

Fowlis, W. W. & Hide, R. 1965. Thermal convection in a rotating annulus of liquid. Effect of viscosity on the transition between axisymmetric and non-axisymmetric flow regimes. *J. Atmos. Sci. 22*, 541.

Fultz, D. & Kaiser, J. A. C. 1971. The disturbing effects of probes in meteorological fluid-model experiments. *J. Atmos. Sci. 28*, 1153.

Fultz, D., Long, R. R., Owens, G. V., Bohan, W., Kaylor, R. & Weil, J. 1959. Studies of thermal convection in a rotating cylinder with some implications of large-scale atmospheric motions. *Meteor. Monogr. 4*, 21.

Hide, R. 1958. An experimental study of thermal convection in a rotating liquid. *Phil. Trans. Roy. Soc. A 250*, 341.

Hide, R. & Mason, P. J. 1970. Baroclinic waves in a rotating fluid subject to internal heating. *Phil. Trans. Roy. Soc. A 286*, 201.

Kaiser, J. A. C. 1969. Rotating deep annulus convection. Part I. Thermal properties of the upper symmetric regime. *Tellus 21*, 789.

Kaiser, J. A. C. 1970. Rotating deep annulus convection. Part 2. Wave instabilities, vertical stratification, and associated theories. *Tellus 22*, 275.

Ketchum, C. B. 1972. An experimental study of baroclinic annulus waves at large Taylor number. *Tellus 29*, 665.

Koschmieder, E. L. 1972. Convection in a rotating laterally-heated annulus. *J. Fluid. Mech. 51*, 637.

McIntyre, M. E. 1968. The axisymmetric convective regime for a rigidly bounded rotating annulus. *J. Fluid Mech. 32*, 625.

Pfeffer, R. L., Fowlis, W. W., Fein, J. & Buckley, J. 1970. Experimental determinations of the transition between the symmetrical and wave regimes in a rotating differentially heated annulus of fluid. *Pure Appl. Geophys. 81*, 263.

Walin, G. 1971. Contained non-homogeneous flow under gravity or how to stratify a fluid in the laboratory. *J. Fluid Mech. 48*, 647.

НЕКОТОРЫЕ ИССЛЕДОВАТЕЛЬСКИЕ ЭКСПЕРИМЕНТЫ С НОВЫМ ТИПОМ ВРАЩАЮЩЕГОСЯ КОЛЬЦЕВОГО СОСУДА С НЕОДНОРОДНО НАГРЕТОЙ ЖИДКОСТЬЮ

Представлены результаты экспериментов с вращающимся неоднородно нагретым кольцевым сосудом. Показано, что при подходящей конструкции сосуда интенсивность зонального бароклинного движения может быть получена не зависящей от основной стратификации плотности. В описываемых экспериментах было найдено, что бароклинная неустойчивость происходит в состоянии, характеризуемом малыми наклонами изотерм. Некоторые особенности наблюдаемых полей течений и температуры, в частности, основная стратификация и наклон изотерм сравниваются с приближенными предсказаниями теории. Обсуждаются определенные фундаментальные трудности, связанные с чувствительностью бароклинного течения к малым изменениям в граничных условиях.